Sequential Kelvin Wave interactions with upper ocean during DYNAMO

Dariusz B. Baranowski[1]
Piotr J. Flatau[2]
Maria K. Flatau[3]

[1] Institute of Geophysics, Faculty of Physics, University of Warsaw
[2] Sripps Institution of Oceanography, UCSD
[3] Naval Research Laboratory, Monterey

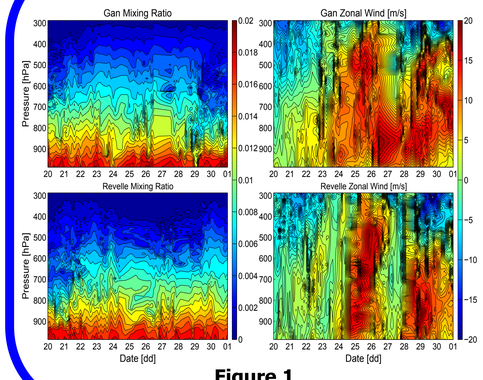

Figure 1

Motivation

During DYNAMO field campaign 3 MJO events were intensively measured. The November 2011 MJO was associated with two sequential atmospheric Kelvin waves. Fig. 1 presents water vapour mixing ratio (left column) and zonal wind speed (right column) from upper soundings launched from Gan (top row) and R/V Roger Revelle (bottom row). Two distinguishable anomalies manifested by strong westerlies in zonal flow represent two sequential atmospheric Kelvin waves. Lag between them is clearly observed at R/V Roger Revelle location. Water vapour mixing ratio contours present mid troposphere humidity variation associated with these waves.

Fig. 2 presents Latent Heat Flux (LHF), ShortWave Flux (SWF) and Wind Speed measured on R/V Roger Revelle (top panel). Bottom panel presents Precipitable Water Vapour (PWV), SeaSnake ocean temperature and precipitation measured at the same location. Presented time period corresponds with November MJO in DYNAMO location, but precipitation pattern (red curve, bottom panel) is divided into two smaller precipitation periods. These two periods correlate with variation in fluxes. During each convective periods increased negative LHF and decreased SWF as well as increased wind speed are observed. Between convective periods, two days of strong solar radiation, decreasing LHF and wind speed are visible. These convective periods match periods of atmospheric Kelvin waves measured by upper soundings at the R/V Roger Revelle location.

During calm, non convective period between sequential atmospheric Kelvin waves, diurnal signal in upper ocean temperature (blue curve, bottom plot) and increase in PWV calculated from upper sounding at the same location are visible.

Here, we study question of importance of diurnal cycle in upper ocean for Kelvin wave propagation.

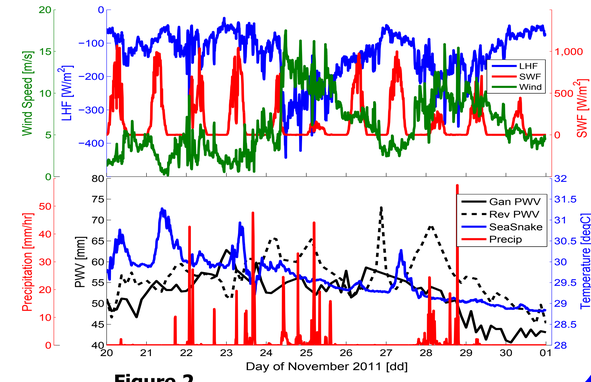

Figure 2

UEA SeaGlider observations

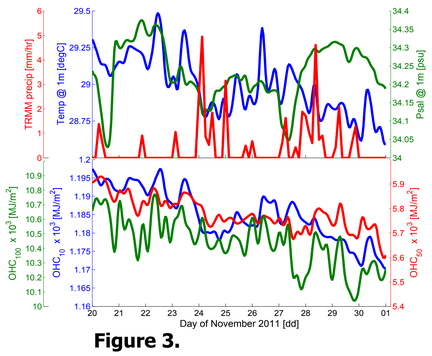

Figure 3.

Upper ocean measurements from UEA SeaGlider instrument that operated between 3S and 4S along 78.8E present similar patterns in temperature to measured at the R/V Revelle location.

Upper panel of Fig. 3 presents temperature (blue) and salinity (green) at 1m depth, and TRMM precipitation at the glider location (red). Presented period again corresponds with November MJO onset.

Bottom panel of the same figure presents Ocean Heat Content (OHC) calculated from ocean surface down to 10m (blue), 50m (red) and 100m (green). One can see decreasing trend of OHC in all layers that correlates with decrease in temperature at 1m depth. Two convective periods are again visible in TRMM precipitation data.

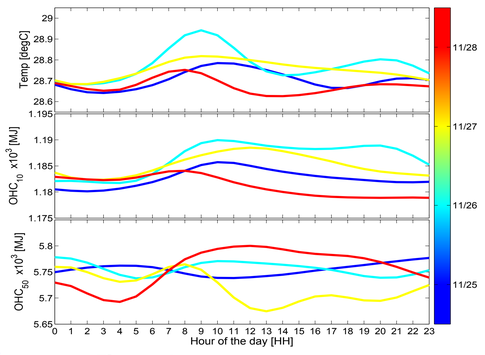

Figure 4.

Fig. 4 shows diurnal temperature variation at 1m depth (top panel), OHC down to 10m (middle panel) and OHC down to 50m (bottom panel) for 4 consecutive days Nov 25 - Nov 28 (blue to red). First day represents the first convective period, last day represents the second convective period, while Nov 26 and Nov 27 represent gap between atmospheric Kelvin waves. It is apparent that diurnal temperature variation as well as increase of OHC in shallow 10m layer is stronger during two calm, non convective days.

Numerical Experiments

Numerical simulations were performed using global shallow water model. Various runs were forced by disturbing mass source centered at the equator at [0,0]. Source had constant spatial distribution with 10 degrees radius. Elsewhere source value was set to 0.

Amount of energy (mass) put into system was conserved between simulations. Each model run was 10 days long, but source was turned on for the first 5 days of simulation only.

Fig. 6 represents our base simulation in which forcing is constant. Color contours represent geopotential anomaly, arrows represent wind anomaly. This set up is the same in all figures presented in this section. In base simulation features similar to forced Kelvin wave, Rossby wave and resulting westerly wind burst are represented.

Our test simulations results are presented in Fig. 7 and Fig. 8. Diurnal cycle in upper ocean is represented in our model by diurnal variation in forcing. For run presented in Fig. 7 this diurnal variation was constant, when for run presented in Fig. 8 it was additionaly disturbed, meaning that for first 2 days diurnal cycle was weaker then in following days.

One can see that key features are still present in both test simulations. We are observing clear Kelvin and Rossby waves response. Difference from base run is in distribution and amplitude of Kelvin waves and intensified westerly bursts between each Kelvin wave. Difference between test simulations is small comparing to the difference with base run.

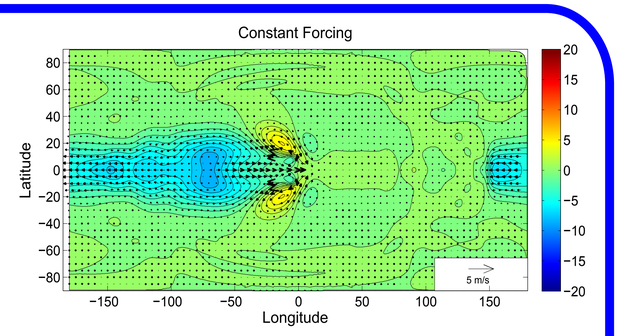

Figure 6

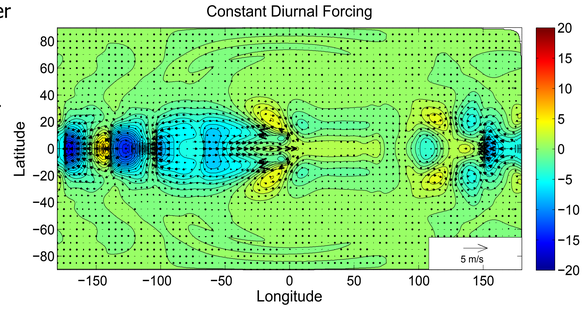

Figure 7

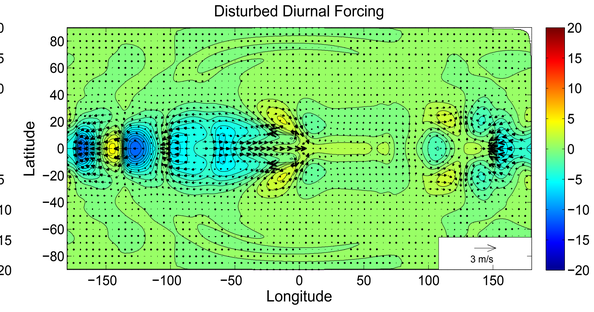

Figure 8

Contact Information:
Dariusz B. Baranowski: ul. Pasteura 7, Warsaw
dabar@igf.fuw.edu.pl

Acknowledgements.
We would like to thank Adrian Matthews for UEA SeaGlider data and Chris Fairall for providing us with fluxes. This work was supported by the ONR DRI grant to Scripps Institution of Oceanography.